1

Silicon Science and Technology as the Background of the Current and Future Knowledge Society

Sergio Pizzini
Department of Materials Science, University of Milano-Bicocca, Milan, Italy

COPYRIGHTED MATERIAL

1.1 Introduction

This introductory chapter aims to present the unique potentialities of semiconductor silicon as the substrate or the component of a variety of devices that support the development of the society in which we live today and where our sons and daughters will live, hopefully, tomorrow; taking, however, as known all the very basic physics concerning the electronic and optical properties of semiconductor silicon as well as the basic concepts concerning silicon devices [1–7]. Also, considering the number of issues that should be taken into consideration to enlighten this critical role of silicon, only a few of these, selected in a very personal, and possibly not entirely objective, manner will be discussed in full detail.

The discussion will start from the thermonuclear synthesis of silicon and will end with the properties and applications of silicon nanodots and nanowires studied today in research labs worldwide, with the consideration that silicon's uniqueness derives from its specific structural, physical and chemical properties, which make elemental silicon readily obtainable from widely diffused raw materials and directly suitable for technological applications in microelectronics, optoelectronics and photovoltaics, without neglecting high-power devices, chemical sensors and radiation detectors.

The analysis will be focused on the variety of its structural forms, which range from single crystal towards microcrystalline, nanocrystalline and amorphous, with a discontinuous change of properties that, in fact, allow a multiplicity of applications.

Advanced Silicon Materials for Photovoltaic Applications, First Edition. Sergio Pizzini.
© 2012 John Wiley & Sons, Ltd. Published 2012 by John Wiley & Sons, Ltd.

Also, the physics of defects in silicon will be briefly taken into consideration, in order to provide insight into its radiation hardness, which makes silicon particularly suitable in hard-radiation environments, like space and the modern hadronic colliders, as well as the role of defect engineering in modern microelectronics and optoelectronics.

Finally, a few advanced applications will be discussed.

1.2 Silicon Birth from a Thermonuclear Nucleosynthetic Process

It is well known that silicon, in the form of silicon compounds, is the main component of the earth's crust, as well as that earth has a liquid iron core. It is instead, probably, not so well known that silicon and iron are the main results of the gravitational collapse of a blue giant, a star at least eight times more massive than our sun [8]. Only with this kind of star might the thermonuclear nucleosynthetic processes driven by gravity and temperature occur within their cores, which succeed, after the combustion of hydrogen, helium and carbon (see Figure 1.1), to reach the formation of silicon (^{28}Si) by fusion of a carbon (^{12}C) and an oxygen nucleus (^{16}O). The nuclear process then proceeds by the fusion of Si to (^{56}Fe) iron. Conditions in the core then become so extreme that electron pressure is overcome and the protons are forced to react with electrons to give neutrons and neutrinos

$$p + e \rightarrow n + \text{neutrino} \quad (1.1)$$

and a neutron star is born (see Figure 1.1).

The rebounding shock wave plus radiation pressure from the escaping neutrinos could also cause the outer layers of the star to explode outwards as a Type-II supernova. This condition causes a massive flux of free neutrons, and the existing nuclei are able to absorb one or more of these neutrons, undergo beta decay, absorb another neutron or neutrons, beta decay, a process that moves nuclei up the periodic table towards and past uranium. This kind of explosion disseminates a cloud of multicomponent dust in the open space, where the dust can aggregate, again under the action of gravity, giving rise to new stars and planets, these last, like the earth, with a light silica and silicate crust and a heavy iron core.

1.3 Silicon Key Properties

1.3.1 Chemical and Structural Properties

Silicon is chemically very active, it reacts in a wide range of temperatures with oxygen, metals and oxides less stable than silicon dioxide (SiO_2)

$$Si + O_2 \rightarrow SiO_2 \quad (1.2)$$

$$Me + Si \rightarrow Me_{Si} \quad (1.3)$$

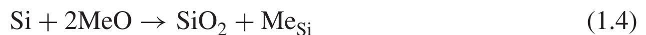

$$Si + 2MeO \rightarrow SiO_2 + Me_{Si} \quad (1.4)$$

(where Me_{Si} is a metallic impurity in a substitutional or interstitial position of the silicon lattice) giving rise to the initial formation of an oxide or a surface alloy. As most of

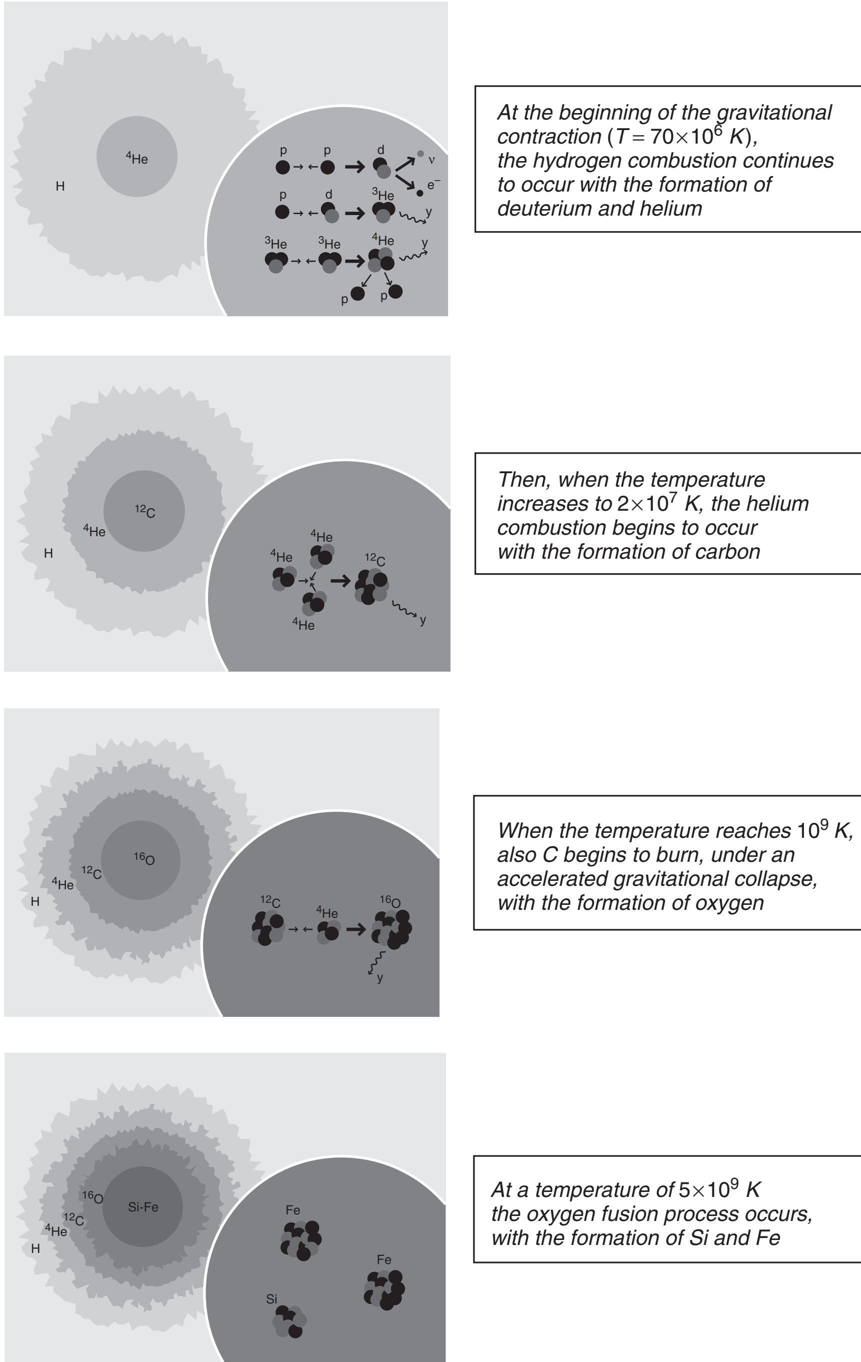

Figure 1.1 *Sequence of events occurring during the final burst of a blue giant star. Reprinted with permission from [8]. Copyright (2009) INFN.*

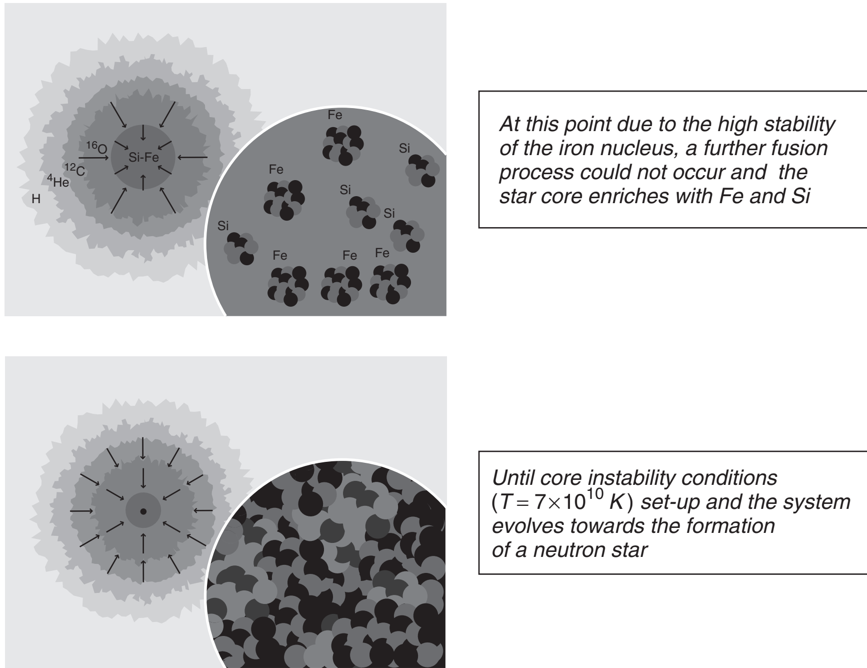

Figure 1.1 *(continued)*

the common oxides are thermodynamically less stable than SiO_2, see Figure 1.2, surface contamination of silicon by interaction with most oxide ceramics is a common event in high-temperature silicon processing.

Subsequent annealing might favor the indiffusion of the metals segregated at the surface, with a definitive bulk alloying. This is one of the main technological problems encountered with silicon growth, wafering and its further processing. Metallic impurities, in turn, generate gap states that might behave as deep recombination centers for electronically or optically injected minority carriers and/or trap levels for majority carriers [9]. A key property of silicon dioxide, which will be discussed in Chapter 4, is its ability, in the form of micrometric or submicrometric precipitates, to getter metallic impurities, where gettering is a process able to trap and electrically inactivate a metallic impurity dissolved in silicon.

Gettering has been [10, 11] and still is, one of the most important applications of defect engineering, a topic and a process technology that has been steadily investigated during the past forty years and brought to success the microelectronic sector [12, 13].

Due to its high thermodynamic stability ($\Delta G^\circ(298\,\mathrm{K}) = -825.30\,\mathrm{kJ/mol}$), its high dielectric constant and its compliance with the silicon surface, silicon dioxide (SiO_2) behaves also as an almost perfect, impervious and electronically nonconducting membrane, which protects the silicon surface from further oxidation, acting also as a nonconducting electronic barrier. It is well known that MOS device development has been possible thanks to this property [4].

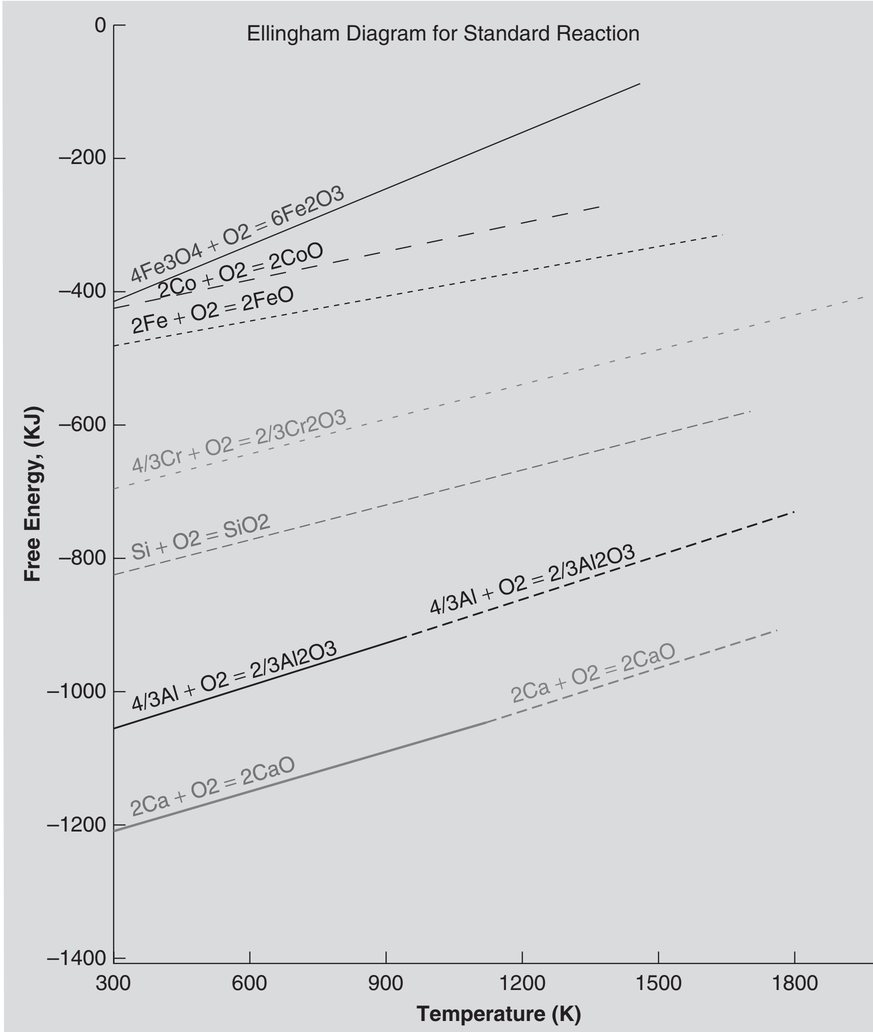

Figure 1.2 *Temperature dependence of the standard free energy of formation of selected oxides: the change of colors in the case of Al and Ca occur at the melting point of the metals (San Josè State University Ellingham diagrams web tool).*

In comparison with compound semiconductors, silicon offers the advantage of being elemental, and therefore, not subject to stoichiometry deviations, which penalize in some cases the success of doping procedures in compound semiconductors.

Differently from most compound semiconductors silicon is environmentally friendly, and it does not present major decommissioning problems at the end of life of any silicon device, including photovoltaic modules.

Depending on its structure at the macro-, micro-, nanolevel, the electronic properties of the material show sensible changes.

Under atmospheric pressure at temperatures below its melting temperature at 1412 °C, independently of its microscopic structure, solid silicon is a semiconductor with a cubic, diamond-like structure.

Under applied mechanical stress, silicon presents a number (at least four) of high-pressure, metastable metallic polytypes [14], with the first phase transition from the diamond structure to that of β-Sn occurring at 20 GPa. A number of additional phases might be obtained by indentation or nanoindentation [15].

In its intrinsic, undoped, state, it presents all the typical fundamental properties of elemental covalent semiconductors in terms of mechanical and thermal properties, band structure, optical properties, resistivity, electron mobility and lifetime [2]. The energy gap of silicon is 1.12 eV wide, almost at the center of the emission spectrum of the sun and therefore very suitable for solar photon harnessing.

It can be easily doped p-type and n-type with acceptor (B, Ga) and donor (P, As, Sb) substitutional impurities during the crystal growth process using a mother alloy, or during device manufacturing process using diffusion and/or ion implantation technologies. Due to the relatively small mobility of dopants, the doping profile remains almost constant during the device lifetime, with a great advantage for the long-term properties of silicon-based devices.

At the nanometric limit, under atmospheric pressure, it behaves, instead, as a quasidirect-gap semiconductor and its properties might be tuned by changing the size of the nanocrystallites, as is shown in Chapter 9.

Under atmospheric-pressure conditions, it can be grown from a liquid charge as a single-crystal ingot with the float zone and Czochralski processes or as a multicrystalline ingot with variants of the Bridgman technique, where the bulk texture depends on the crystallization conditions.

It can also be deposited, from suitable gas phases or plasma atmospheres, using chemical vapor deposition (CVD) techniques, epitaxially on a single-crystal substrate, or on nonsingle-crystal substrates, in microcrystalline, nanocrystalline or amorphous configuration, as is shown in Chapters 7 to 10.

Under specific electrochemical conditions, an array of nanocrystalline silicon dendrites might be created starting from bulk silicon, with the formation of so-called porous silicon (PS) [16–18] that presents peculiar optical emission properties, suitable both for the fabrication of light-emitting diodes (LED) and chemical and biosensors.

Liquid silicon has a metallic behavior and can be stirred by applying an electromagnetic field, with important consequences on its electronic properties after solidification. As an example, electromagnetic stirring is applied in magnetic Czochralski (MCz) growth [19–21] to control the convection flows in the melt, which are largely responsible for the inhomogeneous distribution of dopants and oxygen in the crystal, and, thus, to homogenize their content in the solid ingot. Oxygen, in turn, is one of the most important impurities in solid silicon, for its ability to getter metallic impurities when present in the form of submicrometric precipitates (internal gettering processes (see Chapters 3 and 4)) and to make the material less prone to stress-induced slip during high-temperature processes.

Also, electromagnetic stirring might be applied in directional solidification processes used for the purification of metallurgical silicon in order to favor the segregation of carbon and other impurities [22], as will be shown in Chapter 2.

1.3.2 Point Defects

Under thermodynamic equilibrium conditions, which are never achieved experimentally [23], silicon should contain an equal concentration of thermally generated intrinsic point defects, the self-interstitials and vacancies

$$Si_{Si} \leftrightarrow Si_i + V_{Si} \quad (1.5)$$

Actually, the effective concentration of defects depends on a variety of homogeneous and heterogeneous recombination/trapping reactions at internal and external surfaces, developed during the growth of a silicon ingot and further heat treatments. Three different types of self-interstitials (tetrahedral, hexagonal and dumbbell) populating the crystal, each with peculiar properties, as their mobility and their charge states. Vacancies take five different charge states in the silicon bandgap, ranging from 0.05 eV above the valence band up to 0.7 eV. No gap states are associated with the dumbbell interstitial, which is stable in the Si_i° state, while gap states are associated with the hexagonal and the tetrahedral ones [24]. Both defects, therefore, might be the origin of donors, acceptors or recombination states, depending on the Fermi level.

Due to the large values of their formation enthalpies, which range around 2.4–3 eV for both vacancies and interstitials [25–27] their concentrations are small and very difficult to experimentally measure with classical density methods. Indirect methods like diffusivity measurements or positron annealing spectroscopy [28] are used for vacancies, while diffusivity measurements with interstitially diffusing impurities are used for self-interstitial concentration measurements [29].

Point defects in silicon are easily produced by irradiation. As an example, isolated silicon vacancies and self-interstitials trapped at impurities are generated under irradiation with 1.5–3.0 MeV electrons at 4.2 K and have been identified by EPR spectra [30]. The fact that isolated interstitials could not be found experimentally motivated the conclusion that self-interstitials are mobile, migrating at long distances even at 4.2 K.

It is also well known that point defects interact easily with impurities, with the formation of point defect–impurity complexes, which can be studied and identified with DLTS (deep level transient spectroscopy), TCS (thermally stimulated current) and EPR (electron paramagnetic resonance) [31–34] techniques.

1.3.3 Radiation Damage and Radiation Hardness

It is known that MeV electron irradiation and ion implantation of silicon gives rise to similar defects, where the dominant irradiation defects are vacancy–oxygen pairs and the divacancy, associated with a shallow acceptor center at E_c–0.18 eV and to deeper centers, respectively [35]. Different defects are originated by neutron irradiation, where the damage is dominated by extended defects or defect clusters [36].

Irradiation-induced point defects, point-defect complexes and defect clusters are the main results of the radiation damage, which is severely detrimental for the long-term behavior of both solar cells in space and for silicon detectors used to track the collision patterns in modern hadron colliders [37], see next section.

The main effects on silicon detectors, which are segmented, small-sized pixel silicon diodes, are an increase of the leakage current, an increase of the depletion voltage, an

increase in carrier trapping and inversion. This last problem is caused by the compensation of the donor doping concentration by dominant defects that behave as acceptors.

As a long life associated with low radiation damage is required for silicon detectors in a hadronic collider, work has been done to improve the material stiffness while maintaining the highest device performance.

It has been shown that radiation hardness is significantly improved by the presence of oxygen, which can be a native impurity in Czochralski silicon at a concentration of about 10^{18} at cm^{-3}, and that could be implanted or diffused in float-zone silicon, which would be the preferred solution, as FZ silicon presents the better diode performances due to its intrinsic high resistivity and low recombination center content.

We report in Figure 1.3 the results of neutron, meson and proton irradiation on the concentration of trap levels N_{eff} and of the depletion voltage V_{dep} as a function of the fluence Φ_{eq} for standard float-zone detectors ([O] = 1×10^{15} at cm^{-3}), oxygenated FZ silicon ([O] = 1×10^{17} at cm^{-3}) and Cz silicon ([O] = 1×10^{18} at cm^{-3}). It is very interesting to observe that in oxygenated silicon the damage looks systematically lower than in FZ silicon, caused by the higher stiffness of the oxygenated silicon.

These results confirm the improved radiation hardness to protons of devices made with oxygenated high-resistivity FZ silicon observed by Li *et al.* [36], who showed that oxygenated silicon is advantageous in radiation hardness to gamma and proton irradiation, in terms of detector full depletion voltage degradation, as compared to the control samples. Instead, there is little improvement in radiation hardness to neutron irradiation, which has been attributed to the nature of neutron-induced damage that is dominated by extended defects or defect clusters.

The higher radiation hardness of oxygenated silicon, which is maximum for Co^{60} gamma irradiation, where the point-defect production is predominant, is still under debate, but has been recently associated with the suppression of strongly recombining

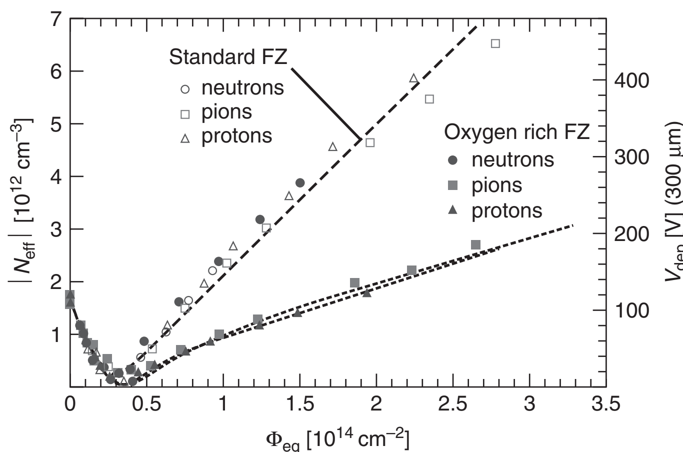

Figure 1.3 *Effect of irradiation with neutrons, pions (light mesons) and 24-GeV protons on the concentration of trap levels and on the depletion voltage (Unpublished results from CERN's RD48 Collaboration). Reprinted with permission from CERN's RD50 Collaboration. Copyright (2011) Michael Moll.*

vacancy-type midgap defects, labeled I defects, which are formed in large concentration in oxygen-lean silicon and that are primarily responsible for the n-type to p-type inversion [38] and by the concentration increase of the IO_2 complex between interstitial silicon and an oxygen dimeric species [39].

Point-defect complexes are generated with any kind of particle irradiation. As an example, by irradiation with MeV protons a vacancy–hydrogen pair has been proposed to be formed [40].

Apart from the impact of light impurities, like hydrogen, carbon, oxygen and of their complexes with point defects on the radiation hardness of radiation detectors, the key role of point defects and of their complexes on the physical properties of silicon is well known. The study of their behavior was, in fact, one of the main subjects of basic and applied research in semiconductor physics over the last thirty years, with thousands of published papers and the establishment of defect-engineering technologies. The role of one of these complexes, the B–O complex, which involves interstitial boron, on the lifetime degradation of solar cells [41], will be discussed in depth in Chapter 3.

1.4 Advanced Silicon Applications

1.4.1 Silicon Radiation Detectors

One of the most challenging questions of modern science is about the origin of our universe, the unification of the physical laws, the discovery of the Higg's boson and about the nature of the dark matter, which constitutes the major part of the universe itself. The experiments now running at the CERN LHC (Large Hadron Collider), after those which were carried out at the CERN's LEP and at the FermiLab's Tevatron Collider, are one of the most exciting attempts of how to approach these questions by the use of proton–proton collisions at energies of 3.5 TeV, (3.5 times higher than at the Tevatron) which correspond approximately to a temperature of 7×10^{20} K, a temperature that occurred in the burning Universe less than one millisecond after the big bang. Incidentally, the possibility is under advanced study at the LHC to quadruple this energy in the next four–six years.

In the LHC, proton–proton collisions generate subatomic particles (mesons, quarks, etc.) whose detection is uniquely possible by the use of arrays of suitable sensors, which not only should detect the event, but should track the particles traversing the detector, thus allowing a measure of the mass and the moment of the generated particles [37].

Silicon has been demonstrated to be the material of choice for tracking detectors, which were already successfully used in the past CERN's experiments as well as at Tevatron, but that are actually the most sensitive part of the machine itself, because of the damage induced by the lattice collisions with high-energy particles (protons, neutrons, mesons) and γ- and X-rays.

As the threshold energy for causing the knock out of a silicon atom from its regular lattice position, forming a vacancy and a self-interstitial, is only 25 eV, eight orders of magnitude lower than the energy of the incident protons in LHC experiments and the protons fluencies are very high (now above 3×10^{14} particles/cm^2 [42] and up to 10^{16} cm^2, in the future very high luminosity colliders [43]), the damage is unavoidable

and the sensors must resist for the entire life of the LHC experiments (six months per year over a period of ten years) as their substitution would be exceedingly costly [44].

Segmented 2D silicon detectors, used in most of the LHC experiments provide excellent submicrometric spatial resolution, while being cost effective, due to well-established very large scale integration (VLSI) technologies used in their fabrication. Radiation detectors have been traditionally fabricated on n-type, high-resistivity float-zone (FZ-Si) wafers, where the high resistivity allows the establishment of full depletion under reasonably low operating voltages.

Since it has been experimentally proven, as shown in the last section, that oxygen improves the radiation hardness of silicon; detectors are nowadays made with oxygenated FZ silicon or with high-resistivity Czochralski silicon.

Figure 1.4 shows the complex configuration of the Atlas experiment's detectors, while Figure 1.5 shows the fine details of one of the first collisions detected at the Atlas experiment.

With the foreseen increase of the luminosity, after the initial phase of the LHC experiments, a new form of silicon sensor whose fabrication makes use of micromachining technology as well as the standard processes of planar technology is requested to satisfy these new severe constraints.

3D sensors, which might fulfill this request, have been fabricated using silicon. In this new configuration, the p^+ and n^+ electrodes penetrate through the silicon bulk, rather than being limited to the silicon wafer surface.

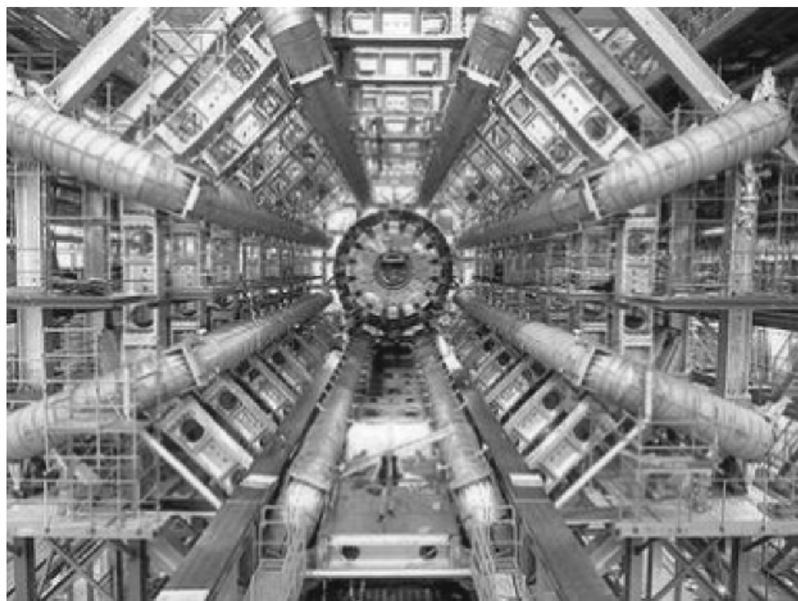

Figure 1.4 *The large (see the person on the center bottom) toroidal magnet supporting the ATLAS experiment at the CERN's LHC in Geneva, aimed at the discovery of the Higgs boson and of supersymmetric particles. Also here, silicon detectors are central for monitoring the traces of the particles formed after a high-energy collision of protons. Reprinted with permission from CERN Courier. Copyright (2011) CERN Courier.*

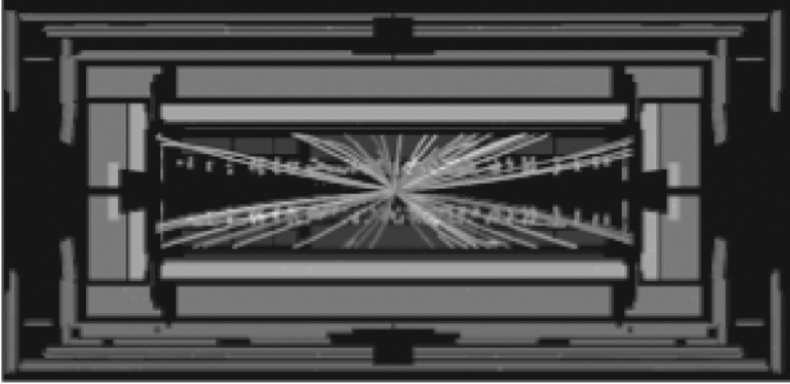

Figure 1.5 One of the first collisions observed at the LHC's Atlas experiment. Reprinted with permission from CERN Courier. Copyright (2011) CERN Courier.

The advantages of 3D design, compared with the traditional planar design, depend on the condition that here the electric field is parallel (rather than orthogonal) to the detector surface, the charge-collection distance can be several times shorter, the collection time considerably shorter, the spatial resolution higher and the voltage needed to extend the electric field throughout the volume between the electrodes (full depletion) an order of magnitude smaller, for 300 μm thick silicon [42]. This technology has many potential applications, for example in extreme radiation environments, luminosity monitors, and medical and biological imaging.

1.4.2 Photovoltaic Cells for Space Vehicles and Satellite Applications

Photovoltaic silicon cells have been used since the late 1950s as viable, efficient (today $>24\%$) and long-lasting power sources for space vehicles and satellites [45]. A specific drawback of silicon solar cells in space is a loss of efficiency, which decreases down to 13% after 15 years, caused by the accumulated radiation dose and consequent radiation damage, which cannot be recovered, like in the case of detectors used in hadronic colliders.

Detailed studies were carried out [46] both by artificial irradiation of silicon solar cells with monoenergetic particles typically present in space radiation (1-MeV electrons and low-energy protons) and by measuring the damage of solar cells carried out by satellites. The problem considered was that the electrons and protons of the Van Allen belt would cause radiation damage to silicon solar cells and a gradual reduction of the power output of solar power plants of satellites passing through the belt. One of the results of this study is that the radiation damage caused by monoenergetic electrons and by monoenergetic protons of various energies has less impact on n-type silicon solar cells than on the commonly used p-type cells.

The damage associated with the irradiation with low-energy protons (150–270 keV) is clearly due to defects generated in the proximity of the p-n junctions, but it could be minimized by suitable protecting layers [47]. More recent results [48] of experiments carried out by irradiation with 1-MeV electrons, at temperature between 80 and 300 K of silicon-based and GaAs-based solar cells have shown that the silicon degradation is strongly

temperature dependent, while it is almost temperature independent in GaAs solar cells. Meanwhile, it emerges that although the density of radiation-induced defects is larger in GaAs than in silicon; the defects in silicon are most effective recombination centers.

1.4.3 Advanced Components Based on the Dislocation Luminescence in Silicon

A different property of point defects in silicon is their ability to coalesce and form microscopic and macroscopic (extended) defects, under form of vacancy clusters and voids for vacancies and dislocation loops, extended interstitials and {311} defects for self-interstitials [49–51].

The presence of dislocations in silicon is normally associated with the simultaneous presence of defect states [52–54], which behave at room temperature as minority-carrier recombination centers, with strong influence on the diffusion length L_d as can be seen, as an example in Table 1.1, which shows that L_d decreases with the increase of the dislocation density N_D, where $L_d = \sqrt{D\tau}$, with D the diffusivity in $\mu m^2/s$ and τ the lifetime in seconds.

For this reason the presence of dislocations and their formation during device processing must be prevented in microelectronic and photovoltaic devices. At low temperatures (12 K) dislocations present, instead, the typical photoluminescence spectrum reported in Figure 1.6, which calls for the occurrence of possibly useful radiative recombination processes.

This property suggested, in fact, the possible use of dislocations as light-emission sources in silicon-based devices, considering that the indirect character of the band to band (BB) transition in crystalline silicon and the systematic BB emission intensity decrease with increasing working temperature would preclude LED or lasing potentialities to bulk crystalline silicon [55].

It was, however, shown that the dislocation luminescence intensity also quenches down on increasing the temperature, as is shown in Figure 1.7 for the case of the D1 line at 0.807 eV ($\lambda = 1.55$ am) which is the most intense among the other three, and the question that arises is whether the temperature-induced light-emission degradation would be intrinsic to the nature of dislocations or result from the interaction of dislocations with light impurities (O, N, H) and metallic impurities.

This further question stimulated a significant interest worldwide, aimed at the understanding the role of light impurities and metals on the dislocation luminescence. Among

Table 1.1 *Effect of the dislocation density on the minority-carrier diffusion length L_D of Cz silicon. The first column reports the initial value of L_D, before any thermal treatment, without or with stress.*

Sample	L_d (as grown) (μm)	L_d (tt 670°C) (μm)	N_D (cm^{-2})
Reference 1	240 ± 20	260 ± 20	–
Reference 2	380 ± 30	370 ± 30	–
D9-1-dislo	300 ± 30	220 ± 20	10^3
D8-1- dislo	230 ± 20	160 ± 20	10^4
D33-1- dislo	370 ± 30	60 ± 6	10^5
D39-1- dislo	390 ± 30	35 ± 3	$\geq 10^7$
D33-2- dislo	370 ± 30	50 ± 5	$\geq 10^7$

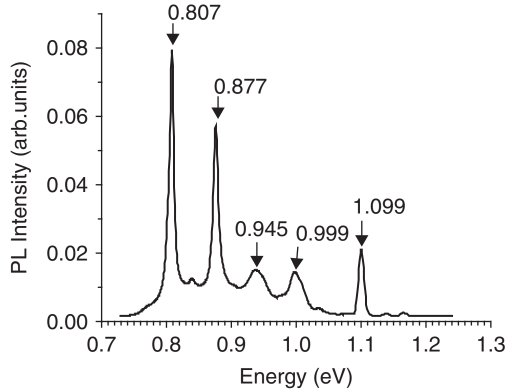

Figure 1.6 *Typical PL spectrum of a dislocated (111)-oriented FZ silicon sample ($T = 12$ K, $N_D = 10^7$ cm^{-2}). The lines at 0.807, 0.877, 0.945 and 0.999 eV are conventionally labeled D1, D2, D3 and D4.*

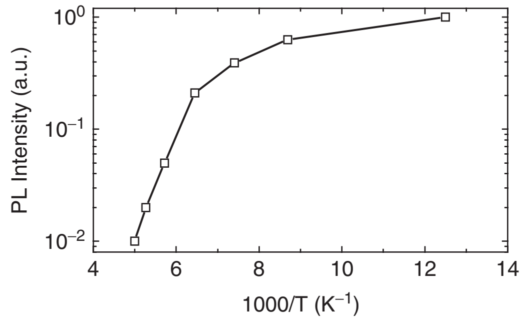

Figure 1.7 *Temperature dependence of the D1 line intensity.*

the wide literature available on this subject, the results of a years-long interlaboratory study could be cited [56], which succeeded in showing the key role of oxygen on the dislocation luminescence, the effect of specific dislocation generation procedures as well as the role of metallic impurities on the dislocation luminescence yield [57–64], leaving open, however, the issue concerning the real potential of dislocations as efficient light sources.

Recent work has, instead, almost conclusively shown, on the one hand, that relatively efficient (0.1–1%), room temperature light-emitting devices could be manufactured using high-quality silicon substrates, proper impurity gettering and passivation techniques and sophisticated device fabrication procedures, capable minimizing the impurity-based non-radiative carrier recombination losses [65, 66].

Also, it has been shown that dislocations might work as the active components of silicon-based light-emitting devices [67], see Figure 1.8, indicating that the thermal quenching of both the Band to Band (BB) and the dislocation photoluminescence is, in fact, induced by nonradiative carrier-recombination processes associated with the presence of residual metallic impurities in the substrate material [68, 69].

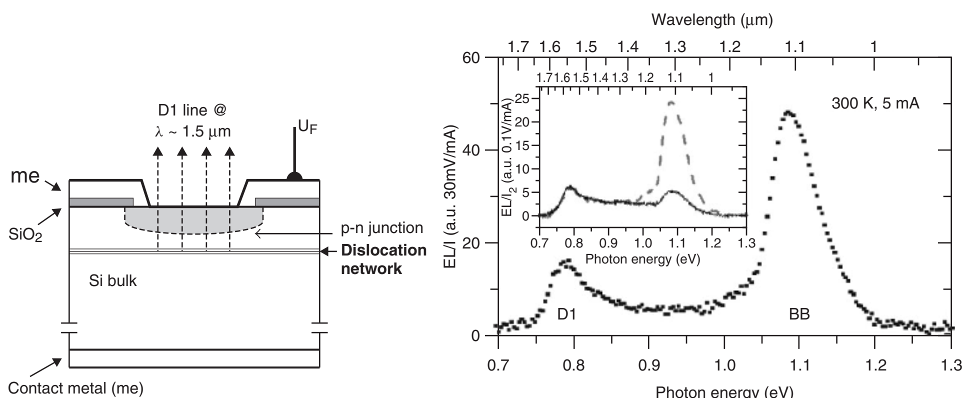

Figure 1.8 *(left) Schematic view of a p-n LED based on the emission at 1.55 μm generated by a dislocation network. (right) Electroluminescence spectrum at room temperature for a 2-mm deep dislocation network yielding an efficiency >0.3% for the line at 1.55 μm and ≅1% for the band to band (BB) line. The insert shows the influence of the distance between p-n junction and dislocation network. Figure on right reprinted with permission from [67]. Copyright 2009, Wiley-VCH.*

The conclusion, however, remains that silicon is a relatively poor room-temperature light emitter and that its BB emission occurs in a range of energies (∼1.1 eV), which is of little applicative interest. The peak energy of the D1 band of dislocations at ca. 0.810 eV would, instead, couple perfectly with the range of optical communications at 1.5μm, and, therefore, light-emitting devices based on the dislocation luminescence could be a viable alternative to the already used Er-doped III-V semiconductor devices, although still requiring adequate technological developments.

An interesting property of dislocations, which looks like an ideal connection between dislocations and silicon nanowires, is their ability to induce a kind of local de-alloying in Si-Ge alloys, which has been experimentally proven by means of photoluminescence measurements at low temperatures (2–20 K) [70]. The samples used, consisted of a Si_{1-x}-Ge_x ($x_{Ge} = 0.34$), 1-μm thick, layer grown on a graded Si-Ge buffer layer, by low energy plasma enhanced chemical vapor deposition. After a rapid thermal annealing ($T = 750$–$1000\,°C$) for different times, the formation of Si-rich and Ge-rich nanowires along the dislocation core was evidenced by the setup of both the silicon dislocation luminescence, with the characteristic D1–D4 lines and the band to band (BB) luminescence of Ge.

1.4.4 Silicon Nanostructures

Silicon nanostructures, consisting of an assembly of nanometric objects with different dimensionalities, are a class of silicon-based materials with electronic and optical properties that depend on both their individual size and spatial distribution. The first identified silicon-based material with nanometric properties was porous silicon (PS) [71], the first also to show room-temperature photo- and electroluminescence in the visible. PS itself consists of an agglomerate of silicon nanowires, which might be formed by a kind

of electrochemical synthesis [72]. One of the main problems of porous silicon is the extremely complex dependence of its luminescence on fabrication, storage and surface treatments [73]. In addition, about two decades after its discovery, the very origin of the luminescence of PS remains still unexplained. When PS is used for devices, other problems emerge, associated with its broad emission band, low external quantum efficiency and long recombination times, albeit the device performance might be definitely improved by the use of dedicated manufacturing techniques [74], with a potential tenfold increase of the peak emission intensity [75].

The discovery of optoelectronic potentialities of nanometric silicon-based materials stimulated the interest towards nanometric structures different from that of PS, also in the prospective to develop silicon-based lasing devices [76] and a new generation of flash memories [77, 78]. The most recent attempts in this direction were devoted to silicon nanocrystals embedded in SiO_2, for which a fairly efficient visible light emission is demonstrated and for which different preparation techniques, fully compatible with the microelectronic technology processes, are already available [79–83]. Also for this material, the origin of its luminescence, consisting typically in a broad Gaussian peak centered at 1.6 eV, much higher in intensity than that expected for bulk silicon, was not entirely understood for years. It is now well demonstrated that two mechanisms operate on silicon nanocrystals, a quantum confinement effect due to the size of the nanocrystals or an emission stimulated by surface defects, the one or the other prevailing, depending on the treatment of the nanocrystals [84].

The potentialities of silicon nanostructures as the active substrates of the third-generation solar cells are discussed in full details in Chapter 10.

Silicon nanowires are a different kind of silicon nanostructure, which are currently fabricated with a number of different techniques [85–88] and with a growing number of preliminary applications not only in microelectronics and photovoltaics.

As an example, their use in lithium/sulfur rechargeable batteries is supposed to represent progress in safety and power density. In these batteries, the anode consists of an assembly of silicon nanowires grown on a stainless steel plate. Here, the silicon nanowires are used for their capacity to insert and extract lithium metal from their structure, without significant failures associated with a 400% volume change [89]. The specific energy of this cell is ~350 Wh/kg, which is already higher than that of commercial Li-ion batteries (335 Wh/kg).

The future application of silicon nanowires in electronic and optoelectronic devices will be, however, only possible if the growth of these nanostructures can be controlled in terms of size and localization in space. Albeit the full technological exploitation of silicon nanocrystals to solar cells, light-emitting diodes and flash memories is still far away, challenges and promises are in good balance.

References

[1] Electronic structure and Properties of Semiconductors, W. Schröter Ed. (1991) in *Materials Science and Technology, A comprehensive Treatment*, Vol. 4 VCH.

[2] *Properties of silicon*, EMIS Data Reviews Series 4 (1988) INSPEC Publ. ISBN 0 85296 475 7, London.

[3] S. Wolf, R. N. Tauber *Silicon Processing for the VLSI Era*, (1986) Lattice Press, California.

[4] E. H. Nicollian, J. R. Brews *MOS (Metal oxide semiconductor) Physics and Technology* (1982) John Wiley & Sons, New York.

[5] S. M. Sze *Semiconductor Devices: Physics and Technology* (2008) 2nd edn, Wiley India Pvt Ltd, India.

[6] A. Luque and S. Hegedus (2003) *Handbook of Photovoltaic Science and Engineering* John Wiley & Sons, Ltd.

[7] T. Markvart and L. Castafier (2003) *Practical Handbook of Photovoltaics: Fundamentals and Applications* Elsevier, UK.

[8] M. Hack, (2009) Alchimie celesti *Asimmetrie* **9**, 12–19.

[9] Landolt Börnstein Numerical Data and Functional Relationships in Science and Technology (1989) Volume 22 Semiconductors, Subvolume b, *Impurities and Defects* Springer Verlag, Berlin.

[10] W. Schröter, E. Spieker, and M. Apel (1995) *Gettering of metal impurities in silicon* Proc. Fifth Workshop on the role of impurities and defects in silicon device processing NRLE/SP-**413–8250**, 85–92.

[11] T. Y. Tan, R. Gafiteanu, and U. M. Gösele (1995) *Toward understanding and modeling of impurity gettering in Si* Proc. Fifth Workshop on the role of impurities and defects in silicon device processing NRLE/SP-**413–8250**, 93–100.

[12] K. A. Jackson (ed) (1996) Processing of Semiconductors, *in Materials Science and Technology, A Comprehensive Treatment*, Vol. 16 VCH.

[13] S. Ashok, J. Chevallier, K. Sumino, and E. Weber (eds) (1992) Defect Engineering in Semiconductor growth, Processing and Device Technology, *MRS Symposium Proceedings* **262**.

[14] J. Z. Hu and I. L. Spain (1984) Phases of silicon at high pressure *Solid State Communications* **51**, 263–266.

[15] B. D. Malone, J. D. Sau, and M. L. Cohen (2008) Ab initio study of the optical properties of Si-XII *Physical Review B* **78**, 161–202.

[16] Z. C. Feng and R. Tsu (1994) *Porous Silicon* World Scientific Books.

[17] L. Canham (ed.) (1997) *Properties of Porous Silicon*, Institution of Engineering and Technology.

[18] L. Pavesi, G. Panzarini, and L. C. Andreani (1998) All-porous silicon-coupled microcavities: Experiment versus theory *Physical Review B* **58**, 15794–15800.

[19] K. Kakimoto and H. Ozoe (2000) Oxygen distribution at a solid-liquid interface of silicon under traverse magnetic field *Journal of Crystal Growth* **212**, 429–437.

[20] M. Mito, T. Tsukada, M. Hozawa, C. Yokoyama, You-Rong Li, and N. Imaishi (2005) Sensitivity analyses of the thermophysical properties of silicon melt and crystal *Measurement Science and Technology* **16**, 457–466.

[21] N. Ma and J. S. Walker (2006) Electromagnetic stirring in crystal growth processes *Fluid Dynamics & Material Processing* **2**, 119–125.

[22] U. Wunderwald, K. Dadzis, M. Zschorsch, T. Jung, and J. Friedrich (2009) *Influence of travelling magnetic field on melt convection during Bridgman type solidification of multicrystalline silicon* Proc. 24th EUPVSEC, 21–25 September, 2009 (Hamburg) pp. 1023–1028.

[23] U. Gösele and T. Y. Tan (1982) The nature of point defects and their influence on diffusion processes at high temperatures *MRS Symposium Proceedings* **14**, 45–59.

[24] G. D. Watkins (1997) Native defects and their interactions with impurities in silicon *MRS Symposium Proceedings* **469**, 139–150.

[25] J. Justo, M. Z. Nazant, E. Kaxiras, V. V. Bulatov, and S. Yip (1998) Interatomic potentials for silicon defects and disordered phases *Physical Review B* **58**, 2539–2550.

[26] R. Car, P. Bloch, and E. Smargiassi (1992) Ab initio molecular dynamics of semiconductor defects *in: Defects in semiconductors 16, Materials Science Forum* **83–87**, 433–446.

[27] L. Colombo, M. Tang, Diaz de la Rubia F., and Cargnoni, (1996) Structure, energetics, clustering and migration of point defects in silicon, *Physica Scripta* **T66**, 207–211.

[28] S. C. Sharma, N. Hozhabri, R. C. Hyer, T. Ossain, S. Kim, F. O. Meyer III, M. F. Pas, and A. Stephens (1992) A study of defects in Czochralski grown silicon by positron annihilation spectroscopy, *MRS Symposium Proceedings* **262**, 45–50.

[29] F. Morehead, F. N. A. Stolwijk, W. Meyberg, and U. Gösele (1983) Self-interstitial and vacancy contributions to silicon self-diffusion determined from the diffusion of gold in silicon *Applied Physics Letters* **42**, 690–692.

[30] G. D. Watkins (1991) Intrinsic point defects in semiconductors in *Materials Science and Technology*, Vol. 4 *Electronic structure and Properties of Semiconductors* W. Schröter (ed) 107–138.

[31] W. Orton and P. Blood (1990) *The Electrical Characterisation of Semiconductors: Majority Carrier Properties (Techniques of Physics)* Academic Press, London.

[32] G. L. Miller, D. V. Lang, and L. C. Kimerling (1977) Capacitance Transient Spectroscopy *Annual Review of Materials Science* **7**, 377–448.

[33] Y. H. Lee, R. L. Kleinhenz, and J. W. Corbett (1977) EPR of a thermally induced defect in silicon *Applied Physics Letters* **31**, 142–144.

[34] M. Pawłowski, R. Kozłowski, and P. Kamiński (2010) EPR studies of MCz-Si and FZ-Si irradiated with high neutron fluence WODEAN Workshop – Bucharest 13–14 May 2010.

[35] L. Vines, E. V. Monakov, J. Jensen, A. Yu. Kuznetsov, and B. G. Svensson (2009) Formation and annealing behavior of point defects in MeV ion implanted n-type epitaxial silicon *Materials Science and Engineering* **B159-160**, 177–181.

[36] Z. Li, B. Dezillie, M. Bruzzi, W. Chen, V. Eremin, E. Verbitskaya, and P. Weilhammer (2001) HTLT oxygenated silicon detectors: radiation hardness and long-term stability *Nuclear Instruments Methods Physics Research* **461**, 126–132.

[37] C. Leroy and P. G. Rancoita (2007) Particle interaction and displacement damage in silicon devices operated in radiation environments *Reports of Progress in Physics* **70**, 493–625 with 416 references.

[38] I. Pintilie, E. Fretwurst, G. Linström, and J. Stahl (2003) Second-order generation of point defects in gamma-irradiated float-zone silicon, an explanation for "type inversion" *Applied Physics Letters* **82**, 2169–2171.

[39] F. Hönniger, E. Fretwurst, G. Lindström, G. Kramberger, I. Pintilie, and R. Röder (2007) DLTS measurements of radiation induced defects in epitaxial and MCz silicon detectors *Nuclear Instruments Methods Physics Research* **A 583**, 104–108.

[40] J. F. Barbot, C. Blanchard, E. Ntsoenzok, and J. Vernois (1996) Defect levels in n-silicon after high energy and high dose implantation with protons *Materials Science and Engineering* **B 36**, 81–84.
[41] V. V. Voronkov, R. Falster, and A. V. Batunina Modelling lifetime degradation in boron-doped Czochralski silicon *Physica Status Solidi A* in press.
[42] C. DaVia (2003) Radiation hard silicon detectors lead the way *CERN Courier*, January 1.
[43] J. Härkönen, E. Tuovinen, P. Luukka, H. K. Nordlund, and E. Tuominen (2007) Magnetic Czochralski silicon as detector material *Nuclear Instruments Methods Physics Research* **A 579**, 648–652.
[44] K. Gill, V. Arbet-Engels, J. Batten, G. Cervelli, R. Grabit, C. Mommaert, G. Stefanini, J. Troska, and F. Vasey (1997) Radiation Damage Studies of Optoelectronic Components for the CMS Tracker Optical Links CERN/LHCC, 97–30.
[45] C. G. Zimmermann, (2010) Materials challenges in photovoltaic energy generation in space *MRS Bulletin*, **35**, 48–54.
[46] F. M. Smits (1963) The degradation of solar cells under Van Allen radiation *IEEE Transactions on Nuclear Science*, **10**, 88–96.
[47] R. L. Statler and D. J. Curtin (1971) Radiation damage in silicon solar cells by low energy protons *IEEE Transactions on Electron Devices* **ED18**, 412–417.
[48] J. C. Burgoin, R. Kiliulis, C. Gonzales, G. Strobl, C. Flores, K. Bogue, and C. Signorini Deep space degradation of Si and GaAs solar cells *Proceedings of the 25th PVSC* May 13–17 1996, 211–214.
[49] P. Alippi, S. Coffa, L. Colombo, and A. LaMagna (2002) From point to extended defects in silicon: a theoretical study in: *Defect Interaction and Clustering in Semiconductors*, pp. 177–202 Scitec Publications Ltd Uetikon-Zuerich
[50] T. Mchedlidze, S. Binetti, A. LeDonne, M. Suezawa, and S. Pizzini (2005) Rod-like defects in CZ-Si investigated by spin resonance and photoluminescence spectroscopies *Physica Status Solidi C* **2**, 1807–1811.
[51] T. Mchedlidze, S. Binetti, A. LeDonne, S. Pizzini, and M. Suezawa (2005) Electric-dipole spin resonance signals related to extended interstitial agglomerates in silicon *Journal of Applied Physics* **98**, 043507.
[52] A. Castaldini, D. Cavalcoli, A. Cavallini, and S. Pizzini (2005) Defect states in Czochralski p-type silicon: the role of oxygen and dislocations *Physica Status Solidi A* **202**, 889–895.
[53] A. Castaldini, D. Cavalcoli, A. Cavallini, and S. Pizzini (2005) Experimental evidence of dislocation related shallow states in p-type silicon *Physical Review Lett*. **95**, 076401.
[54] D. Cavalcoli and A. Cavallini (2007) Electronic states related to dislocations in silicon *Physica Status Solidi C* **4**, 2871–2877.
[55] L. Pavesi (2003) Will be silicon the material of the third millennium? *Journal of Physics: Condensed Matter* **15**, R1169–R1196.
[56] S. Pizzini (2002–2005) Dislocations, extended defects and interfaces at nanoparticles as effective sources of room temperature photo- and electroluminescence in silicon and silicon-germanium [INTAS Project nr. 01-0194 (2002–2005) Dedales: http://intas.mater.unimib.it].

[57] N. A. Sobolev, A. M. Emel'yanov, E. I. Shek, V. I. Vdovin, T. G. Yugova, and S. Pizzini (2002) Correlation between the defect structure and luminescence spectra in monocrystalline erbium implanted silicon *Journal of Physics: Condensed Matter* **14**, 13241–13246.

[58] S. Binetti, R. Somaschini, A. LeDonne, E. Leoni, D. Li, and D. Yang (2002) Dislocation luminescence in nitrogen-doped Czochralski and float zone silicon *Journal of Physics: Condensed Matter* **14**, 13247–13254.

[59] S. Binetti, S. Pizzini, E. Leoni, R. Somaschini, A. Castaldini, and A. Cavallini (2002) Optical properties of oxygen precipitates and dislocations in silicon *Journal of Applied Physics* **92**, 2437–2445.

[60] S. Binetti, A. LeDonne, V. V. Emsev, and S. Pizzini (2003) Effect of high pressure isostatic annealing on oxygen segregation in Czochralski silicon *Journal of Applied Physics* **94**, 74–76.

[61] E. Leoni, S. Binetti, B. Pichaud, and S. Pizzini (2004) Dislocation luminescence in plastically deformed silicon crystals: effect of dislocation intersection and oxygen decoration *European Physics Journal Applied Physics* **27**, 123–127.

[62] E. Leoni, L. Martinelli, S. Binetti, G. Borionetti, and S. Pizzini (2004) The origin of the photoluminescence from oxygen precipitates at low temperature in semiconductor silicon *Journal of the Electrochemical Society* **151**, G866–G869.

[63] O. V. Feklisova, B. Pichaud, and E. B. Yakimov (2005) Annealing effect on the electrical activity of extended defects in plastically deformed p-Si with low dislocation density. *Physica Status Solidi A* **202**, 896.

[64] S. Pizzini, S. Binetti, A. LeDonne, A. Marzegalli, and J. Rabier (2006) Optical properties of shuffle dislocations in silicon *Applied Physics Letters* **88**, 211910.

[65] M. Green, J. Zhao, and A. Wang (2001) Efficient silicon light emitting diodes, *Nature*, **412**, 805–808.

[66] A. M. Emelyanov, N. A. Sobolev, T. M. Mel'nikova, and S. Pizzini (2003) Efficient silicon light emitting diode with temperature stable spectral characteristics *Semiconductors*, **37**, 730–735.

[67] M. Kittler and M. Reiche (2009) Dislocations as active components of novel silicon devices *Advanced Engineering Materials* **11 (4)**, 249–258.

[68] V. Kveder, M. Badylevich, E. Steinman, A Izotov, M. Seibt, and W. Schröter (2004) Room-temperature silicon light-emitting diodes based on dislocation luminescence *Applied Physics Letters*, **84**, 2106–2109.

[69] V. Kveder, M. Badylevich, W. Schröter, M. Seibt, E. Steinman, and A. Izotov, (2005) Silicon light-emitting diodes based on dislocation-related luminescence *Physica Status Solidi A* **202**, 901–910.

[70] L. Martinelli, A. Marzegalli, P. Raiteri, M. Bollani, F. Montalenti, L. Miglio, D. Chrastina, G. Isella, and H. von Kaenel (2004) Formation of strain-induced Si-rich and Ge-rich nanowires at misfit dislocations in SiGe: A model supported by photoluminescence data *Applied Physics Letters* **84**, 2895–2897.

[71] L. T. Canham (1990) Silicon quantum wire array fabrication by electrochemical and chemical dissolution of wafers *Applied Physics Letters* **57**, 1046–1048.

[72] V. Lehmann and U. Gösele (1991) Porous silicon formation, a quantum wire effect *Applied Physics Letters* **58**, 856–858.

[73] K. Esmer and E. Kahyahan (2009) Influence of the alkali metallization (Li, Na and K) on the photoluminescence properties of porous silicon *Applied Surface Science* **256**, 1548–1552.
[74] S. Ossicini, L. Pavesi, and F. Priolo (2004) Light emitting silicon for microphotonics *Springer Tracts in Modern Physics* **194**.
[75] M. Cazzanelli and L. Pavesi (1997) Time resolved photoluminescence of all porous silicon microcavities *Physical Review B* **56**, 15 264–15271.
[76] S. Furukawa and T. Miyasato (1988) Quantum size effects on the optical band gap of microcrystalline Si:H *Physical Review B* **38**, 5726–5729.
[77] S. Godefroo, M. Hayne, M. Jivanescu, A. Stesmans, M. Zacharias, O. I. Lebedev, G. Van Tendeloo, and V. V. Moshchalkov (2008) Classification and control of the origin of photoluminescence from Si nanocrystals *Nature Nanotechnology* **3**, 174–178.
[78] T. Z. Lu, M. Alexe, R. Sholz, V. Talalaev, R. J. Zhang, and M. Zacharias (2006) Si nanocrystals based memories: effect of the nanocrystal density *Journal of Applied Physics* **100**, 014310.
[79] L. Tsybeskov (1998) Nanocrystalline silicon for optoelectronic applications *MRS Bulletin* **23**, 33–38.
[80] L. Pavesi, L. DelNegro, C. Mazzoleni, G. Franzò, and F. Priolo (2000) Optical gain in silicon nanocrystals *Nature* **408**, 440–444.
[81] M. Zacharias, J. Heitmann, R. Scholz, U. Kahler, M. Schmidt, and J. Bläsing (2002) Size-controlled highly luminescent silicon nanocrystals: A SiO/SiO_2 superlattice approach *Applied Physics Letters* **80**, 661–663.
[82] A. Zimina, S. Eisebitt, W. Ebherardt, J. Heitmann, and M. Zacharias (2006) Electronic structure and chemical environment of silicon nanoclusters embedded in a silicon dioxide matrix *Applied Physics Letters* **88**, 163103.
[83] S. Mirabella, R. Agosta, G. Franzò, I Crupi, M. Miritello, R. Lo Savio, M. A. Di Stefano, S. Di Marco, F. Simone, and A. Terrasi (2009) Light absorption in silicon quantum dots embedded in silica *Journal of Applied Physics* **106**, 103505.
[84] U. Gösele (2008) Shedding new light on silicon *Nature Nanotechnology* **3**, 134–135.
[85] J. L. Liu, Y. Lu, Y. Shi, S. L. Gu, R. L. Jiang, F. Wang, and Y. D. Zheng (1998) Fabrication of silicon nanowires *Applied Physics A:* **66**, 539–541.
[86] Yi Cui and C. M. Liebe (2001) Functional nanoscale electronic devices assembled using silicon nanowire building blocks *Science* **291**, 851–853.
[87] E. Garnett and P. Yang (2010) Light trapping in silicon nanowire solar cells *NanoLetters* **10**, 1082–1087.
[88] D. Buttard, L. Dupré, T. Bernardin, M. Zelsmann, D. Peyrade, and P. Gentile (2004) Confined growth of silicon nanowires for the realization of low cost solar cells, *Physica Status Solidi A* **201**, R11–R14.
[89] Y. Yang, M. T. McDowell, A. Jackson, J. J. Cha, S. Sae Hong, and Yi Cui (2010) New nanostructured Li_2S/silicon rechargeable battery with high specific energy *NanoLetters* **10**, 1486–1491.